THE FERMI SURFACE OF TIN

N. E. ALEKSEEVSKIĬ, Yu. P. GAĬDUKOV, I. M. LIFSHITZ, and V. G. PESCHANSKIĬ

Institute of Physics Problems, Academy of Sciences, U.S.S.R.

Submitted to JETP editor June 17, 1960

J. Exptl. Theoret. Phys. (U.S.S.R.) 39, 1201-1214 (November, 1960)

Possible topological shapes of the Fermi surface of tin are discussed. The most probable shape of the Fermi surface of tin is chosen by comparison with the experimental results of galvanomagnetic measurements.

IT has been concluded from an experimental investigation of the galvanomagnetic properties of tin that this metal has a Fermi surface of the open type.[1,2] The Fermi surface of a metal with tetragonal crystal lattice can in principle be of the "corrugated cylinder," "corrugated plane," or "three-dimensional grid" type, unlike metals with cubic structure for which the first two types are excluded.[3-5]

The experimental data obtained for tin[1,2] pertain mainly to samples with axes located in the principal crystallographic planes. It was possible to conclude from these data that the [100], [010], and [110] directions are open for the Fermi surface of tin. However, to explain all the topological features of the Fermi surface of tin, it was necessary to carry out a more detailed investigation of the anisotropy of the resistance of tin single crystals in large magnetic fields. It was also desirable to consider in greater detail the possible types of Fermi surfaces of metals with tetragonal lattices.

1. ANALYSIS OF GEOMETRY OF FERMI SURFACES FOR CRYSTALS WITH TETRAGONAL STRUCTURE

To investigate the topological features of the constant energy surfaces of metals with tetragonal crystal lattices, we use the following expression for the dispersion of $\epsilon(\mathbf{p})$:

$$\varepsilon(\mathbf{p}) = A_0 - A_1\cos\frac{cp_z}{\hbar} - A_2\cos\frac{cp_z}{2\hbar}\left(\cos\frac{ap_x}{2\hbar}+\cos\frac{ap_y}{2\hbar}\right) - A_3\cos\frac{ap_x}{2\hbar}\cos\frac{ap_y}{2\hbar} - A_4\left(\cos\frac{ap_x}{\hbar}+\cos\frac{ap_y}{\hbar}\right). \quad (1)$$

Here c is the period of the lattice in the direction of the [001] tetragonal axis, and a is the period in the direction of the [100] and [010] binary axes. This expression represents the first harmonics of the Fourier series of the periodic function $\epsilon(\mathbf{p})$ for the tetragonal lattice of the metal.* We do not discuss here the question of the genesis of the spectrum, and in this connection we consider a priori the constants $A_0, \ldots, A_4$ to be arbitrary.

For values of ϵ close to minimum, the constant-energy surfaces are ellipsoids. The position of the centers of these ellipsoids depends on the relation between the coefficients A_i. For example, if all $A_i > 0$, then the centers of the closed constant-energy surfaces $\epsilon(\mathbf{p}) = \epsilon_{min} + \delta\epsilon$ ($\delta\epsilon$ is small) coincide with the origin. As ϵ increases, the volumes of the constant-energy surfaces increase, and at a certain value $\epsilon = \epsilon_1$ (where $\epsilon_1 = A_0 - A_1 - 2A_4 + A_3$) the surface becomes tangent to the faces of the first Brillouin zone.

If the coefficient A_1 is the largest of the A_i, then the surface (1) will in the first place be tangent to the (100) and (010) planes. When $\epsilon > \epsilon_1$ surface (1) is an open surface comprising a plane grid of "corrugated cylinders" parallel to the [100] and [010] axes. For sufficiently large values of ϵ surface (1) will also become tangent to the (111) planes of the Brillouin zone.

If the relations between the coefficients A_i are different (if A_2 and A_3 are greater than the coefficients A_1 and A_4), the surface (1) will with increasing ϵ become tangent to the (111) planes of the Brillouin zone earlier than to the (100) and (010) planes. If the Fermi surface of indium were open it would intersect the (111) planes of the Brillouin zone, somewhat similar to the Fermi surface of gold or copper. (The lattice constant a and the nearest neighboring atoms are $\frac{1}{2}(a_2 + c_2)^{1/2}$ apart. Therefore $A_2 > A_1$ and $A_3 > A_4$.)

*If the coefficients of the Fourier series decrease with increasing number of the harmonic (which is true in the approximation of the strongly-bound electrons), it is sufficient for the analysis of the topology of the constant-energy surfaces $\varepsilon(\mathbf{p}) = \varepsilon$ to retain several of the first harmonics in $\varepsilon(\mathbf{p})$.

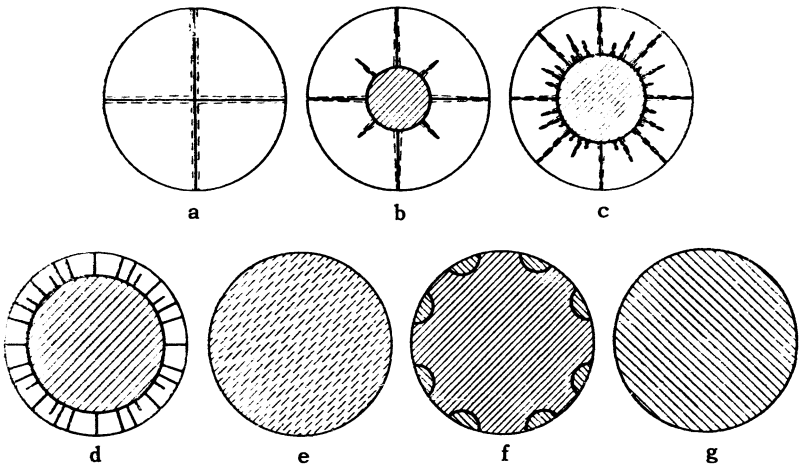

FIG. 1. Transformation of stereographic projections of the special directions of the magnetic field with increasing ε for Fermi surfaces of metals with tetragonal structure of crystal lattice.

If A_4 is the largest among the coefficients A_i, then constant-energy surfaces (1) of the "corrugated cylinder" type are possible. This case takes place when c is much greater than a. However, no metals exist in nature with such a-tetragonal structure.

The edge of the elementary crystal cell of the tin lattice in the direction of the [001] axis is much smaller than the edge of the cell in the [100] direction ($a/c \approx 1.8$). We therefore assumed that the coefficients A_i satisfy the inequalities

$$A_1 > A_2 > A_3 > A_4. \qquad (2)$$

For the sake of simplicity, we shall assume that all $A_i > 0$, and investigate in detail the constant-energy surfaces described by equation (1)* with relation (2) for the coefficients A_i.

If $(\epsilon - \epsilon_{min}) < 2(A_2 + A_3)$, the surfaces (1) are closed. If $(\epsilon - \epsilon_{min}) > 2(A_2 + A_3)$, the surface (1) will be an open surface comprising a plane grid of "corrugated cylinders."

At not too large values of ϵ, the average direction of the open trajectories $\epsilon = \text{const}$, $p_z = \text{const}$ is located in the (001) plane. With increasing ϵ, the diameters of the "corrugated cylinders" increase, and the surface (1) recalls a pair of "corrugated planes" connected by tubes in the [001] direction. With increasing ϵ these tubes become narrower and narrower, and can in general vanish before the surface (1) touches the (111) faces of the Brillouin zone (if A_1 is much greater than the individual coefficients A_2, A_3, or A_4). If A_1 differs little from A_2, A_3 or A_4, then the tangency of the surface (1) with the (111) faces of the Brillouin zone will take place earlier than the vanishing of the openings in the "corrugated planes." In this case, along with open trajectories in (001), there will exist open trajectories parallel to the [001] axis. (It must be noted that for certain directions of the magnetic field, open trajectories will exist simultaneously with different average directions.)

When ϵ is close to ϵ_{max} the surfaces (1) are closed surfaces located around the points of intersection of the three planes (100), (110), and (111) (and their like).

Figure 1 shows the transformation of the stereographic projections of the directions of the magnetic field which lead with increasing ϵ to open plane sections $p_z = \text{const}$ of the constant-energy surface (1).

If A_1 differs greatly from A_2, A_3 or A_4 (for $A_1 > 2A_2$), then the case f on Fig. 1 will not take place. The surface (1) will be a "corrugated plane" with openings at $2(A_2 + A_3) < (\epsilon - \epsilon_{min}) < 4A_2$. When $(\epsilon - \epsilon_{min}) > 4A_2$, the surface (1) degenerates into two solid "corrugated sheets." When $(\epsilon - \epsilon_{min}) \geq 2A_1$, these sheets form new pairs (i.e., "corrugated planes" joined by tubes), and as ϵ increases the transformation of the stereographic projections proceeds in reverse order from g to d, c, b, and a.

If these "corrugated planes" are pairwise interconnected by straight circular cylinders, then the boundary of the two-dimensional shaded region on the stereographic projections b, c, and d can be accurately calculated. Let d and h be the diameter and the height of the cylinder, b the re-

*In the approximation of strongly-bound electrons, the dependence of the energy on the momentum for tin has a somewhat different closed form

$$\varepsilon(\mathbf{p}) = A_0 + A\cos\frac{cp_z}{\hbar} \pm B\left[\cos^2\frac{ap_x}{4\hbar}\cos^2\frac{ap_y}{4\hbar}\cos^2\frac{ap_z}{4\hbar} + \sin^2\frac{ap_x}{4\hbar}\sin^2\frac{ap_y}{4\hbar}\sin^2\frac{cp_z}{4\hbar}\right]^{1/2}. \qquad (1a)$$

Naturally, each of the two branches of the function (1a) can be expanded in a Fourier series similar to (1), and the surfaces (1) and (1a) are equivalent in their topological properties. (The coefficients A_i in (1) are different for the different branches.)

ciprocal lattice constant in the [100] direction; then, when $\theta < \theta_0$, the open trajectories exist for any value of the angle φ (θ and φ are the angular coordinates of the vector **H**, with θ reckoned from [001]. θ_0 is determined from the condition

$$\tan\theta_0 = h/d. \quad (3)$$

We note that when $\theta < \theta_0$ there exist, along with the open trajectories, closed trajectories with different directions about the electrons, and when $\theta > \theta_0$ only closed trajectories with like directions exist.

When $\theta > \theta_0$ the open trajectories exist only for rational directions of the projections **H** on the (001) plane, i.e., when $\tan\varphi = n/m$ (n and m are integers). The maximum value of the angle $\theta_{n,m}$, at which open trajectories still exist, is obtained from the following condition (n/m is an irreducible fraction)

$$\tan\theta_{n,m} = \frac{\tan\theta_0}{1 - b/d\sqrt{n^2+m^2}}. \quad (4)$$

2. DETERMINATION OF THE DIRECTIONS OF PLANE SECTIONS OF THE OPEN FERMI SURFACE

To estimate the agreement between the surfaces considered above and the experimental data, it is necessary to analyze not only the stereographic projections of the special directions of the magnetic field, but also the open directions, which can be obtained by investigating the dependence of the resistance on the angle between the current and the crystallographic axes at a fixed direction of the magnetic field.

Several types of such current diagrams $\rho_{\mathbf{H}=\text{const}}(\alpha)$ are possible, where α is the angle between the current and the open section, or a certain crystallographic direction ($\mathbf{J} \perp \mathbf{H}$):

1. If for a specified direction of the magnetic field there exists a layer of open trajectories with a single average direction, then the dependence $\rho_{\mathbf{H}=\text{const}}(\alpha)$ will have the following form

$$\rho_{\mathbf{H}=\text{const}}(\alpha) = AH^2\cos^2\alpha + B. \quad (5)$$

When $\alpha = \pm\pi/2$, the current diagram has a minimum, in the direction of which the resistance reaches saturation. For all the remaining angles the resistance will increase without limit in the magnetic field: $\rho \sim H^2$.

2. If for a given direction of the magnetic field there are no open trajectories at all, or there are isolated open trajectories, and $V_1 = V_2$, then the resistance for any value of α increases quadratically with the field. By V_1 and V_2 we mean the following expressions [see Eq. (25) in reference 3]:

$$V_1 = \int S_1(\varepsilon_1, p_z)\,dp_z, \qquad S_1 = \oint p_x \frac{\partial p_y}{\partial\tau}\,d\tau > 0; \quad (6)$$

$$V_2 = -\int S_2(\varepsilon_1, p_z)\,dp_z, \qquad S_2 = \oint p_x \frac{\partial p_y}{\partial\tau}\,d\tau < 0. \quad (7)$$

Here it must be noted that for closed Fermi surfaces the volume compensation is not an accident of low probability, but a regular phenomenon. For metals with even valence a small overlap of the bands should always cause the appearance of compensation of the volumes V_1 and V_2. However, attention must be called to the fact that even for open Fermi surfaces we can speak of relative volumes (in p space within the limits of one cell of the reciprocal lattice) with energy $\epsilon > \epsilon_0$ and $\epsilon < \epsilon_0$, i.e., of "electrons" and "holes" respectively. Therefore, in the absence of open trajectories, the compensation of the volumes V_1 and V_2 is just as regular as in the case of closed surfaces. But in the presence of open trajectories the corresponding expressions in the kinetic coefficients do not reduce to those volumes, and consequently the effects connected with volume compensation do not take place.

3. If, for a given direction of the magnetic field, there exists a layer of open trajectories with different average directions, or there are no open trajectories at all, and $V_1 \neq V_2$, then the resistance reaches saturation in the magnetic field for any value of the angle α.

Thus, the polar current diagrams make it possible to explain the cause of the quadratic increase in resistance for a given direction of the magnetic field, to show whether it is due to compensation of volumes ($V_1 = V_2$) or to the presence of open trajectories, and to determine the directions of the latter.

When speaking of volume compensation, we have in mind the integrals (6) and (7), taken over entire sheets of the Fermi surface. This means that the compensation can take place either spontaneously in the case of an open surface, or as a result of addition with volumes of supplementary surfaces, if such exist.

It is of interest to clarify the character of the variation of resistance on approaching special directions of the magnetic field (at which open trajectories appear or disappear, see Fig. 3 in reference 4). We speak here of the specific case when the compensation of volumes V_1 and V_2 takes place for field directions at which only closed trajectories exist, and consequently there

is a quadratic increase in the resistance for all angles α.

The formulas of reference 4 cannot be used in this case directly in the vicinity of singular points, but their analysis makes it possible to obtain the following expression for ρ:

$$\rho = \rho_0 \frac{D\cos^2\alpha + \lambda_1\gamma_0^2}{[(\Delta V/V + cD)^2 + c'D]\,\gamma_0^2 + \lambda\gamma_0^4}, \qquad (8)$$

where $\Delta V = V_1 - V_2$, and $V = (V_1 + V_2)/2$, c, c', λ, λ_1 are quantities of the same order of magnitude; D is of the same order of magnitude as the thickness of the layer of open trajectories $-\Delta p_z/b\hbar$. When the thickness of the layer of open trajectories vanishes ($D = 0$), we get $\Delta V = 0$.

Let us consider two cases

1) An entire layer of open trajectories ($D \neq 0$) occurs in a special direction of the magnetic field, and there are near this direction strongly elongated closed trajectories. (This case recalls somewhat the case of a "corrugated cylinder" type of surface.)

When $D \neq 0$ the values V_1 and V_2 "become uncompensated," and the resistance can be represented as follows (for $\mathbf{H} \perp \mathbf{J}$)

$$\rho \approx AH^2\cos^2\alpha + B.$$

If the direction of the magnetic field deviates noticeably from the special direction $\theta_1 \gg \gamma_0$ (θ_1 is the angle between **H** and the special direction), then $\rho = \lambda_1 H^2/\lambda$.

Near the special direction ($\theta_1 \lesssim \gamma_0$) there are no open trajectories of the type indicated above, but the presence of strongly stretched out closed trajectories, passing through many cells (on the order of $1/\gamma_0$) of the reciprocal lattice, does not make it possible to attain compensation of V_1 and V_2, owing to the fact that ρ cannot be expanded in powers of γ_0 in this region (see references 3–5).

As a result of the fact that over a very small angle interval ($\theta_1 \sim \gamma_0$) a change takes place in the analytic expression for the resistance as a function of the angle $\rho(\vartheta)$ (ϑ is the angle of rotation of the magnetic field in a plane perpendicular to the current), a very narrow resistance extremum should be observed. The relative magnitude of this extremum is independent of the magnitude of the magnetic field, and the half-width diminishes with increasing magnetic field as 1/H.

2) Let us consider another case of a special direction of the magnetic field, in which the thickness of the layer of open trajectories vanishes. These special directions correspond to the boundary between the two-dimensional regions of the direction of the magnetic field, in which there are open trajectories, and the region of directions of the magnetic field in which there are no open trajectories and $V_1 = V_2$. In the region of magnetic-field directions for which only closed trajectories exist

$$\rho = \rho_0\lambda_1 H^2/\lambda H_0^2 + C, \qquad (9)$$

and in the region of field directions for which there are open trajectories, the resistance in the two extreme cases is of the following form:

$$\rho = AH^2\cos^2\alpha + B, \quad \theta_1 \gg \gamma_0^2;$$
$$\rho = \rho_0\lambda_1 H^2/\lambda H_0^2 + C, \quad \theta_1 \ll \gamma_0^2. \qquad (10)$$

When open trajectories exist, the volumes V_1 and V_2 do not compensate each other, but $\Delta V/V \approx \theta_1$. Therefore, for magnetic field directions with which open trajectories exist in a very narrow region ($\Delta\theta_1 \sim \gamma_0^2$) near $\theta_1 = 0$ we can assume, as before, that $\Delta V = 0$ in the expression for ρ. In this case, a very sharp kink should be observed in the angular dependence $\rho(\vartheta)$.

$$d\rho/d\vartheta = \Lambda H^4\cos^2\alpha + \Lambda_1 H^2. \qquad (11)$$

3) Finally, it should be noted that in a two-dimensional region of directions of the magnetic field $\Delta V/V$ is a monotonic function of the angle θ_1, whereas the thickness of the layer of open trajectories Δp_z vanishes at the center and at the boundary of the two-dimensional region. We can therefore expect ρ to have an additional maximum, which is not sharp, and which is located somewhere inside the two-dimensional region.

3. EXPERIMENTAL RESULTS AND DISCUSSION

The samples were made from a batch of tin obtained by zone melting in the Technology Division of the Institute of Physics Problems, U.S.S.R. Academy of Sciences.* Single crystals were made by several methods: by the Czochralski method, by the Bridgeman method, and also by electric erosion from a bulk single-crystal block. The diameters of the samples ranged from 1 to 2 mm. For measuring the Hall emf, cylindrical samples as well as single-crystal plates measuring 12 × 4 × 0.3 mm were used.

The orientations of the samples were determined optically with an accuracy of ± 1°. The samples were mounted in accordance with the remarks made in reference 6. The anisotropy of the resistance of single crystals of tin was investigated in a magnetic field up to 34 koe at 4.2°K.

*The authors take this opportunity to thank N. N. Mikhaĭlov and L. N. Vasil'ev for the preparation of very pure metal.

TABLE I

Sample	Orientation* φ; ϑ′	$\rho_{300°K}/\rho_{4,2°K}$	Sample	Orientation φ; ϑ′	$\rho_{300°K}/\rho_{4.2°K}$
Sn-1	0°; 0 ° [001]	11 200	Sn-20	24°; 68°	62 500
Sn-2	0°; 26°	14 500	Sn-21	12°; 64°	57 000
Sn-3	0°; 36°	11 100	Sn-22	32°; 62°	49 600
Sn-4	0°; 51°	13 600	Sn-23	23°; 52°	64 000
Sn-5	0°; 62° [011]	11 000	Sn-24	22°; 50°	42 000
Sn-6	0°; 71°	10 800	Sn-25	33°; 48°	46 500
Sn-7	0°; 83°	10 800	Sn-26	37°; 44°	55 000
Sn-8	0°; 90° [010]	48 300	Sn-27	22°; 43°	~60 000
Sn-9	7°; 90°	48 500	Sn-28	4°; 41°	~60 000
Sn-10	15°; 90°	54 000	Sn-29	30°; 39°	~60 000
Sn-11	24°; 90°	45 000	Sn-30	17°; 37°	~60 000
Sn-12	32°; 90°	38 600	Sn-31	12°; 35°	64 500
Sn-13	38°; 90°	47 400	Sn-32	26°; 35°	50 600
Sn-14	45°; 90° [110]	24 200	Sn-33	38°; 35°	~50 000
Sn-15	45°; 71°	55 000	Sn-34	12°; 32°	~50 000
Sn-16	45°; 53°	45 800	Sn-35	20°; 29°	~50 000
Su-17	45°; 41°	44 000	Sn-36	24°; 28°	~50 000
Sn-18	45°; 36°	40 600	Sn-37	38°; 28°	~50 000
Sn-19	45°; 23°	66 700	Sn-38	22°; 26°	~60 000

*φ and ϑ′ are the polar coordinates of the axes of the samples: φ is measured from the (010) or (100) plane, and ϑ′ is the angle between the [001] axis and the axis of the sample. The directions of the axes of the samples are noted on the stereographic projection in Fig. 4a.

All the measurements were made for the case **H ⊥ J** (**J** is the measuring current).

The data on the samples are listed in Table I. For all the tin samples, polar resistance diagrams $\rho_{\mathbf{H}=\text{const}}(\vartheta)$ were obtained in a constant magnetic field H = 23.5 koe.

The diagram of the sample Sn-1 is an eight-folium rosette, on which the resistance minima are observed along the directions [010] and [110] (see Fig. 1 in reference 1). For the same directions a clearly pronounced saturation of resistance is observed in the magnetic field.

For the tin specimens whose axes make a small angle with the [001] axis ($0° < \vartheta' \lesssim 30°$), the resistance diagrams retain in general the shape of eight-folium rosettes, although the relative depths of the minima decrease, and some maxima become smoother. All the minima observed on the resistance diagrams for these samples lie on the line in which the plane of rotation of the magnetic field intersects the (010) and (110) planes. An investigation of the dependence of $\rho(H)$ in the direction of the minima has shown that the saturation of resistance is observed only in samples whose axes lie in the (010) or (110) planes (corresponding to $\varphi = 0°$ and $\varphi = 45°$), and only for those minima, whose directions coincide with the direction of the line of intersection of the final rotation of the magnetic field with the plane passing through the axis of the sample and the [001] axis.

As the angle between the axis of the samples and the crystallographic [001] axis is increased (the angle ϑ′ changes approximately from 30° to

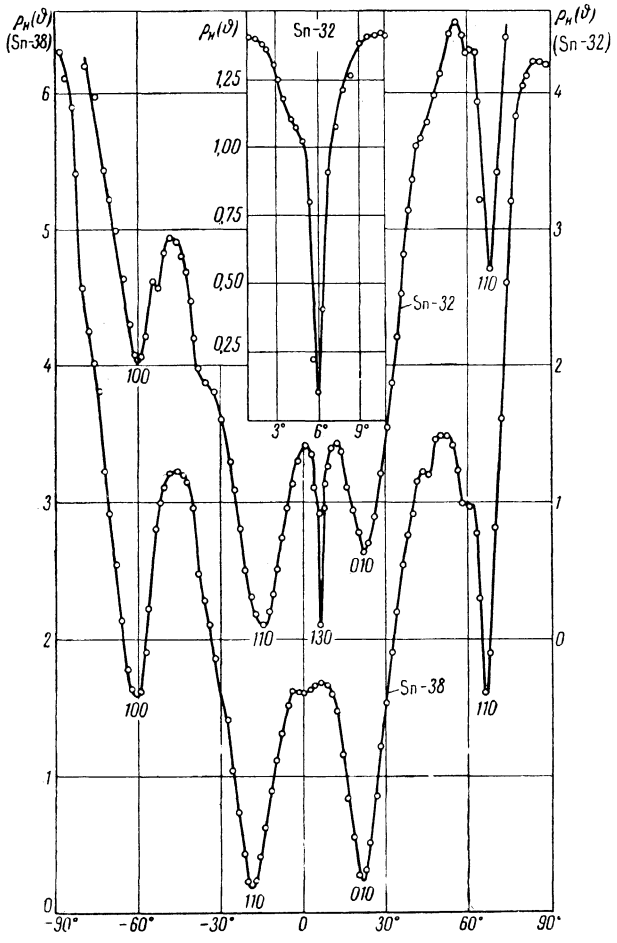

FIG. 2. Polar resistance diagrams in a constant magnetic field H = 23.5 koe for the single crystals Sn-32 and Sn-38 and T = 4.2°K. The values $\rho_{H=\text{const}}(\vartheta)$ are plotted in arbitrary units. The upper curve is the narrow minimum ($\vartheta_{min} = 6°$) for Sn-32, plotted on a larger scale.

50°), there appears on the diagrams $\rho_{H = const}(\vartheta)$ a series of new very narrow and deep minima. The directions of these minima coincide with the directions of the lines of intersection of the plane of the magnetic field with the planes of type (120), (130), (150), and (230). As ϑ' is increased, the first to appear is a minimum in the direction of the (130) plane ($\vartheta'_{(130)} \approx 29°$) (see Fig. 2), after which appear minima in the planes (120) ($\vartheta'_{(120)} \approx 38°$) and (150) ($\vartheta'_{(150)} \approx 37°$), and, finally, in the (230) plane ($\vartheta'_{(230)} \approx 43$?).

In spite of the considerable depth of these minima, no resistance saturation in the magnetic field could be observed for them. This may be explained by the fact that the minima are very narrow, and it is quite probable that an averaging of the resistance over the angle ϑ takes place here. [It should be noted that the widths of all the observed minima decrease (from $\sim 20°$ to $\sim 1°$) with increasing sum of the indices of the corresponding planes.]

The polar resistance diagrams of the samples of tin, for which the angles $\vartheta' \gtrsim 50°$, are in the form of bifoliate rosettes. The changeover from the resistance maximum to the minimum is smooth. The direction corresponding to the minimum on the resistance diagrams coincides in this series of samples with the direction of the line of intersection of the plane of rotation of the magnetic field with the plane passing though the axis of the sample and the [001] crystallographic axis. In the direction of such a minimum, $\rho(H)$ has the form of a saturation curve. For most samples, we investigated also the dependence of the resistance on the magnetic field in directions not coinciding with the directions of the minima. For these directions the resistance increases without limit in a magnetic field, following a nearly-quadratic law.

Figure 3 shows the variation of the form of the polar diagrams of resistance (in the most interesting region of the angles ϑ) with deviation of the sample axis from the [001] axis. Two circumstances must be noted: a) the change from the diagram of the Sn-27 type to the diagram of the Sn-25 type occurs for different angles φ at different angles ϑ'. Thus, it was qualitatively established that the values of ϑ' are approximately 45, 50, and 55° for $\varphi = 0$, 22, and 45° respectively; b) in the polar resistance diagrams of tin samples with the angle ϑ' close to 90°, two additional weekly pronounced minima are observed (at $\vartheta \approx \pm 40°$ and at $\vartheta \approx \pm 17°$).

Table II lists certain characteristic details of polar diagrams of resistance of all the investigated single crystals of tin. All the observed minima are plotted on the stereographic projection shown in Fig. 4 b and c.

The large number of samples of different orientation has made it possible to plot current diagrams of resistance and to draw conclusions concerning the causes of the square-law increase in the resistance or its saturation for different directions of the magnetic field. In the construction of the current diagrams of resistance $\rho_{H = const}(\alpha)$, the diagrams $\rho_{H = const}(\vartheta)$ have been reduced to a single scale. Examples of typical current diagrams are shown in Fig. 5.

The current diagram I (lower curve) is encountered only once for a field direction $\mathbf{H} \parallel [001]$. In this case for any orientation of the current ($\mathbf{H} \perp \mathbf{J}$) the resistance in large fields is almost independent of the magnitude of the magnetic field. It follows, therefore, that there are no open sections of the Fermi surface for this direction of the field (however, one cannot exclude here the existence of isolated open sections), and the volumes V_1 and V_2 do not compensate each other.

The current diagram II (central curve) is characteristic of the directions of the magnetic field located in the planes (010) and (110) (for all angles θ) and in the planes (150), (130), (120), and (230); here the angle θ for the orientations of $\mathbf{H}$ is limited in the following manner: $\theta_{(130)} \lesssim 61°$; $\theta_{(150)} \lesssim 53°$, $\theta_{(120)} \lesssim 52°$, and $\theta_{(230)} \approx 47°$. [It must be noted that the angle $\theta_{(230)}$ is obviously not a maximum, since it was impossible to establish convincingly the vanishing of the minimum in these directions on the $\rho_{H = const}(\vartheta)$ diagrams.] In addition, a current diagram of type II is observed for magnetic field orientations occupying an entire region (over the angles φ and θ) centered about the [001] axis. The boundary of this region was determined only approximately, and only three points are known for it (with not very great accuracy): 1) $\varphi = 0°$, $\theta \approx 45°$; 2) $\varphi = 22°$, $\theta \approx 40°$, 3) $\varphi = 45°$, $\theta \approx 35°$. Similar current diagrams should exist for those magnetic-field directions, for which open sections of the Fermi surface exist. Knowing the direction of the maximum (or minimum) on the current diagram, we can determine the average direction of these sections. An analysis of the experimental data has shown that all the open sections of the Fermi surface of tin are located in the basal (001) plane.

For all the remaining directions of the magnetic field, current diagrams of the third type (upper curve) are observed. These diagrams are characterized by a quadratic increase of the resistance in the magnetic field for any current

TABLE II

Sample	Positions of the minima and maxima (in degrees) on the diagrams $\rho_{H=const}(\vartheta)$*; the parentheses contain the ratio of the resistance for the given value of the angle and the resistance at the lowest minimum	$\Delta\rho_H/\rho_0$ in the direction of the lowest minimum
Sn-1	0 [010] (1); ±33(127); ±45[110] (3)	5.5
Sn-2	0 (1); ±22(45); ±26(44); ±30(45); ±43(19); ±65(93); ±90(37)	10
Sn-3	0 (1); ±12(44); ±15(41); ±25(67); ±40(40); ±52(150); ±70(142); ±75(143); ±90(86)	6
Sn-4	0(1); ±8 и ±18 (small minima) ; ±26(31); ±30(30); ±78(92); ±90(87)	7.5
Sn-5	0(1); ±25(12); ±29(10); ±78(34); ±88(33); ±90(37)	8
Sn-6	0(1); ± 19(66); ± 24(57); ± 82(203); ± 90(197)	8
Sn-7	0(1); ± 17(28); ± 22(25); ± 82(102); ± 90(100)	20
Sn-8	0(1); ± 18(150); ± 25(90); ± 90(420)	
Sn-9	0(1); ± 15(200); ± 25(125); ± 90(450)	
Sn-10	0(1); ± 15(65); ± 24(40); ± 90(165)	
Sn-11	0(1); ± 17(10); ± 23(9); ± 90(35)	
Sn-12	0(1); ± 17(42); ± 23(26); ± 90(110)	
Sn-13	0(1); ± 16(250); ± 22(132); ± 32(320); ± 35(185); ± 90(550)	40
Sn-14	0(1); ± 16(210); ± 22(143); ± 35(365); ± 43(320); ± 90(490)	27
Sn-15	0(1); ± 70(355); ± 75(335); ± 80(385); ± 90(360)	6
Sn-16	0(1); ± 82(1500); ± 90(1440)	10
Sn-17	0(1); ± 14(420); ± 17(300); ± 30(600); ± 35(500); ± 80(1860); ± 90(1230)	9
Sn-18	0(1); ±19(140); ±21(120); ±24(195); ±26(60); ±29(200); ±78(550); ±90(300)	20
Sn-19	0(1); ± 17(158); ± 42(24); ± 78(280); ± 90(100)	58
Sn-20	0(1); ± 39(56); ± 40(65); ± 42(56); ± 90(110)	
Sn-21	0(1); ± 90(550)	50
Sn-22**	0(1); + 20(430); + 25(400); — 87(2600)	24
Sn-23**	0(1); + 53(112); + 54(100); + 60(112); ± 90(185)	160
Sn-24**	0(1); + 16, + 23 and + 26 (minute minima) ; + 85(262)	72
Sn-25	— 48(415); — 46(523); — 35(239); — 34(264); — 29.5(170); — 29(165); —19.5 (121); — 19(105); — 9.5(32); — 9(27); 0(1); + 2(7.5) + 2.5(1.5); +7.5(24); + 8(18); + 15.5(73); +16(68); +21(157); +22(118); +30(209); + 30.5(197); + 35(285); + 37(274); + 68(652); + 70(630); + 90(1000)	
Sn-26**	— 44 (32); — 38(34); — 31(14); — 26 (25); — 6(1); + 5(8.5); + 8(3); +10 (7.5); + 15(3); + 22(12.5); + 28(9)	
Sn-27**	—18(35); —7(77); —3(8); 0(45); +4(1); +9(36); +10(6); +12(50); +18(25)	
Sn-28	— 83(156); — 71(168); — 35(49); — 33(54); — 11(5); — 7(18); —6(5.5); — 5,5(18); + 3(1); + 13(27); + 13.5(23); + 14(28); + 18(16.5); + 31(77); +40(68); + 74(185)	
Sn-29**	—88(78); — 70(40); — 58(45); — 39(24); — 38(28.5); — 20(8.2); — 16(10); —13(7); — 12(8.7); — 8(1,5); — 3,5(7); — 3(2.6); + 1(10); + 12(1); +30(20,5); + 35 (14)	
Sn-30	— 70 (133); — 57(155); — 22(27); — 10(53); — 2(1); + 2(33); + 13(7.8); +26(100); + 28(70); + 30(100); + 46(117); + 55(102); + 79(246)	
Sn-31	— 87(900); — 60(1340); — 30(275); — 13(556); — 5(55); 0°(380); + 10(1); + 25(486); + 25.5(147); + 26(490); + 38(685); +53(466); + 75(1690)	10
Sn-32	— 60(19); — 48(26); — 15(1); 0(13); + 6(1); + 10(13); + 22(5.7); + 55(39); + 69(26); + 86(62)	
Sn-33	— 82(39); from — 75 to —69(66); —32(12,5); —22(20); —16(13); —12 (17); +6(1); + 35(28); + 45(22); + 85(84)	
Sn-34	— 76(200); — 60(310); — 30(63); — 13(131); — 8(100); — 6(14,5); — 3(97); + 10(1); + 25(140); + 26(57); + 26,5(145); + 37(186); + 53(115); + 78(428)	
Sn-35**	— 22(1); — 3(11); 0(4,5); + 2(11); + 17(1,5);	
Sn-36	— 64(2,7); —48(6.5); — 20(1); + 4(4); + 21(1.1); + 48(9.8); + 66(4.5); + 88(7.5)	
Sn-37**	— 47(133); — 36(274); —8(1); + 18(226); + 32(116); + 67(583)	
Sn-38	— 62(8); — 46(16); — 19(1); + 4(8); + 6(8,5); + 21(1.3); + 54(17.5); +66(8); + 86(31)	

*For $\vartheta = 0$ we chose the direction of the line of intersection of the plane of rotation of the magnetic field with the plane passing through the axis of the sample and the [001] axis.

**Samples for which the diagrams $\rho_{H=const}(\vartheta)$ have not been fully investigated.

orientation. Thus, for these directions of the magnetic field there are no open sections of the Fermi surface, and the resistance increases as H^2 because $V_1 = V_2$.

The appearance of additional maxima on the polar diagrams of the samples, the angle ϑ' of which is close to 90°, is probably due to the circumstances mentioned in Article 3 of Sec. 2.

On the basis of an analysis of the diagrams $\rho_{H = const}(\vartheta)$ and $\rho_{H = const}(\alpha)$, a stereographic projection was plotted for the special directions of the magnetic field for the Fermi surface of tin (Fig. 4d). This projection is significantly supplemented by a stereographic projection of the

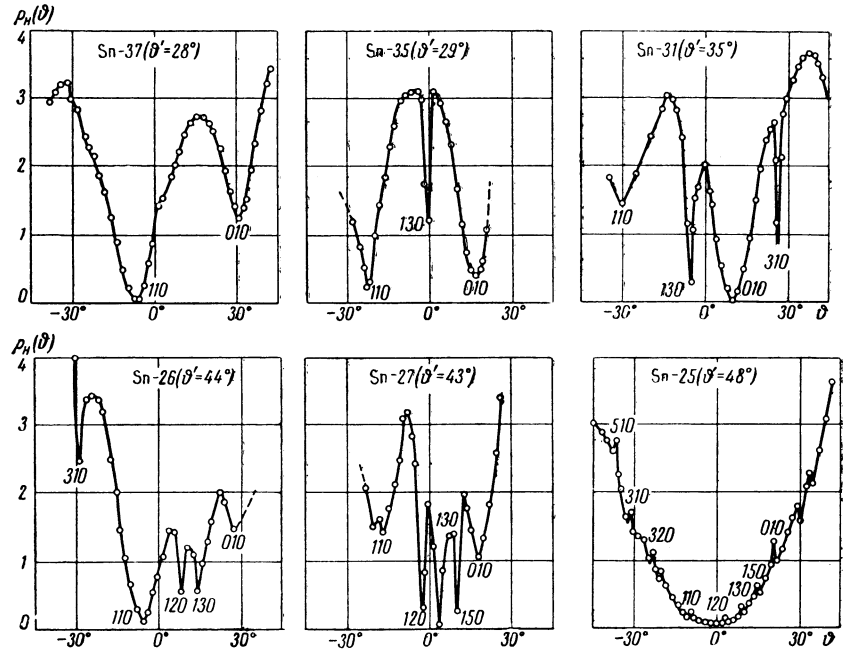

FIG. 3. Variation of the form of the polar diagrams of resistance in a constant magnetic field H = 23.5 koe for a single crystals of tin with increasing ϑ. The values $\rho_{H=const}(\vartheta)$ are in arbitrary units.

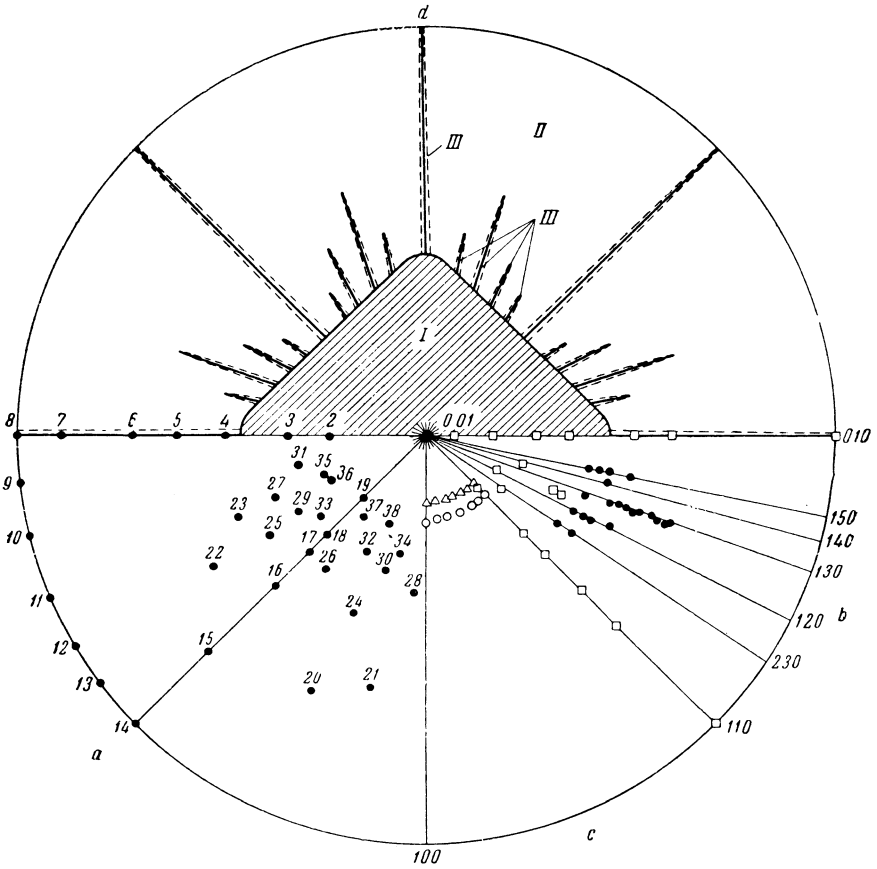

FIG. 4. Stereographic projections. a – directions of the axes of the investigated tin samples (the numbers label the points); b – directions of the minima on the polar resistance diagram; □ – minima for which $\vartheta = 0$; ● – narrow minima; c (○ and △) – directions of weakly-pronounced additional broad minima and maxima; d – special directions of the magnetic field for the Fermi surface of tin: region I – two-dimensional region of magnetic field directions for which open trajectories exist (the thickness of the layer of open trajectories vanishes on the boundary of region I and in the [001]); there are no open trajectories in region II, and the "electron" and "hole" volumes compensate each other, $V_1 = V_2$; regions III are those regions of magnetic-field directions, for which strongly elongated trajectories exist and the compensation of the volumes is violated, $V_1 \neq V_2$. Open trajectories occur only for those directions of the magnetic field which lie on the axial lines.

average directions of the open sections of the Fermi surface of tin, which is a circle with a center corresponding to the [001] direction.

According to the previously employed terminology,[4] region I on Fig. 4d is the two-dimensional region of the directions of the magnetic field, for which open sections of the Fermi surface exist. The special directions are here the center of the region (direction [001]) and the boundary of the region. For these special directions of **H**, the thickness of the layer of the open trajectories vanishes.

In regions II there are no open sections of the Fermi surface and $V_1 = V_2$. For regions III there

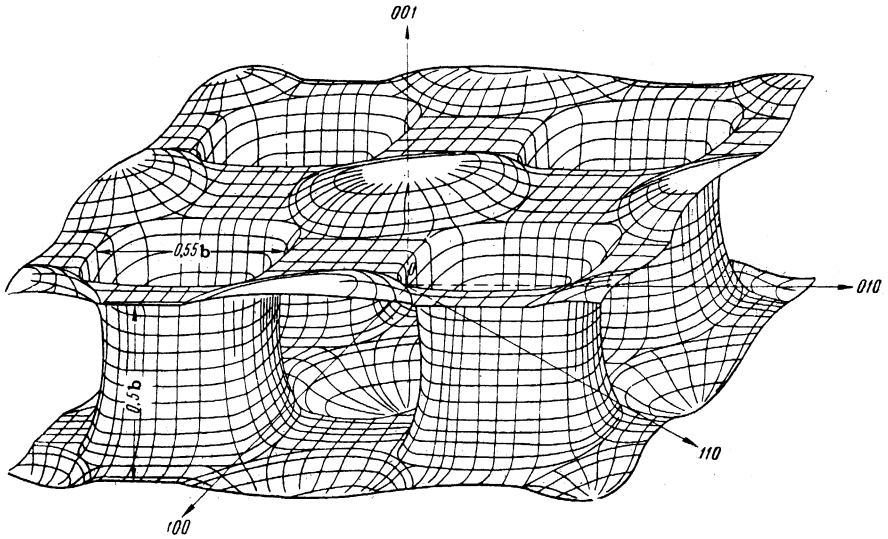

FIG. 6. Open Fermi surface of tin.

exist strongly elongated closed sections [the open sections appear only when the direction **H** is located along the central line — planes with rational indices (100), (110), (120), (130), (150), and (230)].

4. THE FERMI SURFACE OF TIN

The stereographic projection shown in Fig. 4d can be set in correspondence with the Fermi surface comprising a network of "corrugated cylinders" the axes of which coincide with the directions [010], [100], and [110]. Such a surface is topologically equivalent to two corrugated planes, parallel to the (001) plane and joined by tubes, the axes of which have the same direction as the [001] of the reciprocal lattice of tin (Fig. 6).

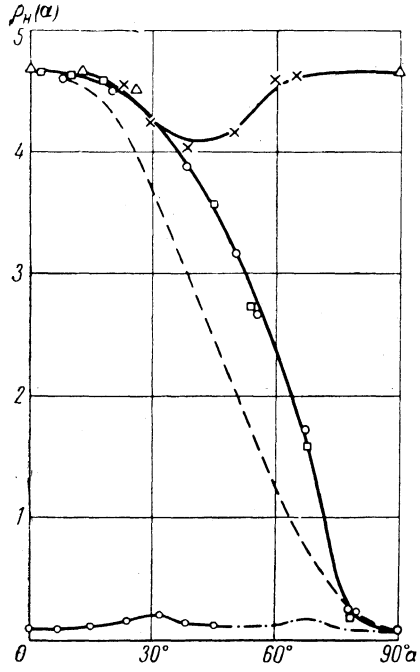

FIG. 5. Typical current diagrams for single-crystal tin; H = 23.5 koe, T = 4.2°K (α is the angle of rotation of the measuring current **J** in the plane perpendicular to the fixed direction of the magnetic field). The experimental curves were obtained for different orientations of the magnetic field: o — **H** ∥ [010]; □ — **H** ∥ [110]; × — field in direction determined by the angles $\varphi = 22°$, $\theta = 90°$; Δ — field in direction $\varphi = 32°$, $\theta = 90°$ (with this, $\alpha = 90°$ when **J** ∥ [001]); lower curve — **H** ∥ [001] (with this $\alpha = 0°$ when **J** ∥ [010]). The dashed line is the curve of $\cos^2 \alpha$.

However, such a surface alone cannot explain the current diagrams of type III (Fig. 5). As was already noted, such a current diagram is obtained in the case of volume compensation ($V_1 = V_2$). In this connection it is necessary to assume that tin has still other constant-energy surfaces, the presence of which makes it possible to obtain such a volume compensation. We assume that at least two branches of the energy spectrum $\epsilon(\mathbf{p})$ are very important for the Fermi surface of tin.

The second isoenergetic surface can be either closed or open. Both versions of the Fermi surface of tin can be reconciled with the stereographic projection of the special directions of the magnetic field (Fig. 4d). If it is assumed that the Fermi surface of tin consists of two surfaces of equal volume, one of which is open and the other closed, then the measurements of the Hall emf* in the [001] direction make it possible to conclude that the open surface is a "hole" surface and the closed one is an "electron" surface.

The experimental results allow us also to estimate some of the parameters of the open Fermi surface of tin. The form of the two-dimensional region I, and the relation between the angles $\theta_{n,m}$ on the stereographic projection (Fig. 4d) indicate that the form of the tubes (bridges between the planes) of the Fermi surface of tin do

*A more detailed description of the results of the measurements of the Hall emf for single crystals of tin will be published soon in JETP.

TABLE III

φ	$\theta_0(\varphi)$, deg	$\theta_{n,m}(\varphi)$, deg.	$d(\varphi)$	$h(\varphi)$
[150]	41	53	0.57	0.5
[130]	38	61	0.57	0.46
[120]	37	52	0.62	0.46
[230]	36	47?	0.93?	
[010]	45		0.52	
[110]	46		0.64	

not differ greatly from straight cylinders. Therefore, to estimate the distance between the planes and the "diameter" of the tube we can use relations (3) and (4). The results of the calculations are given in Table III. The quantities $d(\varphi)$ and $h(\varphi)$ are given in units of the reciprocal lattice constant of tin, b (in the direction [010]). The boundary value θ_{230} could not be established for the [230] direction. In the calculations for the [010] and [110] directions we put respectively $h \approx 0.5$ and $h \approx 0.45$. The data of Table III were used to plot the open Fermi surface of tin (Fig. 6). The presence of two Fermi surfaces in tin ("electron" and "hole") sharply distinguishes the character of the anisotropy of the resistance of tin in a magnetic field from the anisotropy of the resistance of copper, silver, and gold, which also has open Fermi surfaces, made of "corrugated cylinders." A quadratic increase of the resistance in the magnetic field predominates in tin, whereas saturation predominates in copper, silver, and gold. This excludes the possibility of obtaining a linear increase of resistance in polycrystalline tin when averageing in a magnetic field (Kapitza's law).

It should also be noted that the assumption that the Fermi surface is multifoliate can explain the specific features of the galvanomagnetic properties of lead, cadmium, zinc, and other metals, which have open Fermi surfaces.[2]

In conclusion, we consider it our pleasant duty to thank Academician P. L. Kapitza for continuous attention and interest in this investigation.

[1] N. E. Alekseevskiĭ and Yu. P. Gaĭdukov, JETP 36, 447 (1959), Soviet Phys. JETP 9, 311 (1959).

[2] N. E. Alekseevskiĭ and Yu. P. Gaĭdukov, JETP 37, 672 (1959), Soviet Phys. JETP 10, 481 (1960).

[3] Lifshitz, Azbel', and Kaganov, JETP 31, 63 (1956), Soviet Phys. JETP 4, 41 (1957).

[4] I. M. Lifshitz and V. G. Peschanskiĭ, JETP 35, 1251 (1958), Soviet Phys. JETP 8, 875 (1959).

[5] I. M. Lifshitz and V. G. Peschanskiĭ, JETP 38, 180 (1960), Soviet Phys. JETP 11, 131 (1960).

[6] Alekseevskiĭ, Brandt, and Kostina, JETP 34, 139 (1958), Soviet Phys. JETP 7, 96 (1958).

Translated by J. G. Adashko
227